SEVENTH FRAMEWORK PROGRAMME
STRONGGRAVITY
EU FP7-SPACE research project 312789 2013 - 2017

The coronal parameters of local Seyfert galaxies

Andrea Marinucci
(Roma Tre)

on behalf of the
NuSTAR AGN Physics WG

The Extremes of Black Hole Accretion
European Space Astronomy Centre (ESAC)
June 8, 2015

Overview

- Brief introduction on high-energy cutoff measurements
- Nearby AGN seen by NuSTAR
- Results
- Conclusions and future perspectives

- Brief introduction on high-energy cutoff measurements
- Nearby AGN seen by NuSTAR
- Results
- Conclusions and future perspectives

Introduction

One of the main open problem for AGN is the nature of the primary X-ray emission.

It is due to Comptonization of soft photons, but the geometry, optical depth and temperature of the emitting corona are largely unknown

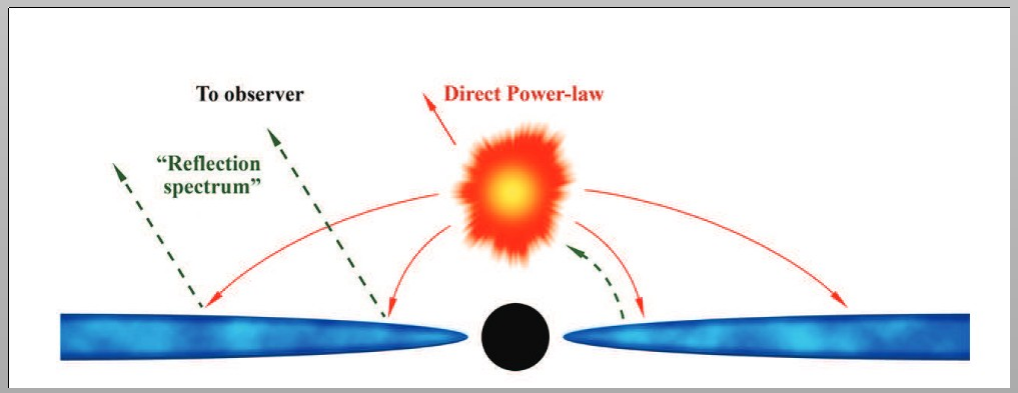

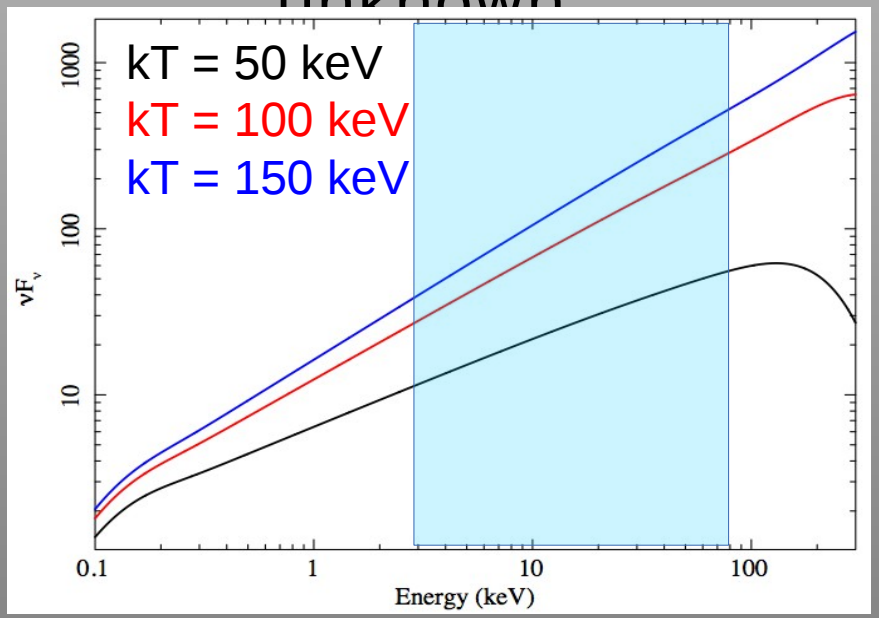

Most popular models imply E_{cut}=2-3x kT_e, so measuring E_{cut} helps constraining Comptonization models.

Introduction

Since the primary X-ray radiation illuminates the disc and is partly reflected towards the observer's line of sight it is fundamental to properly take it into account: Xillver (Garcia+13), Kyreflionx (see Svoboda's poster) .

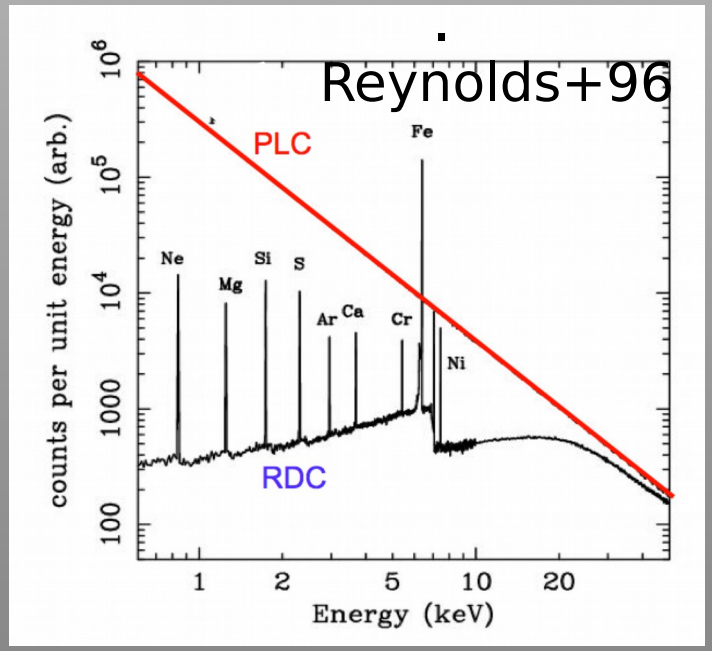

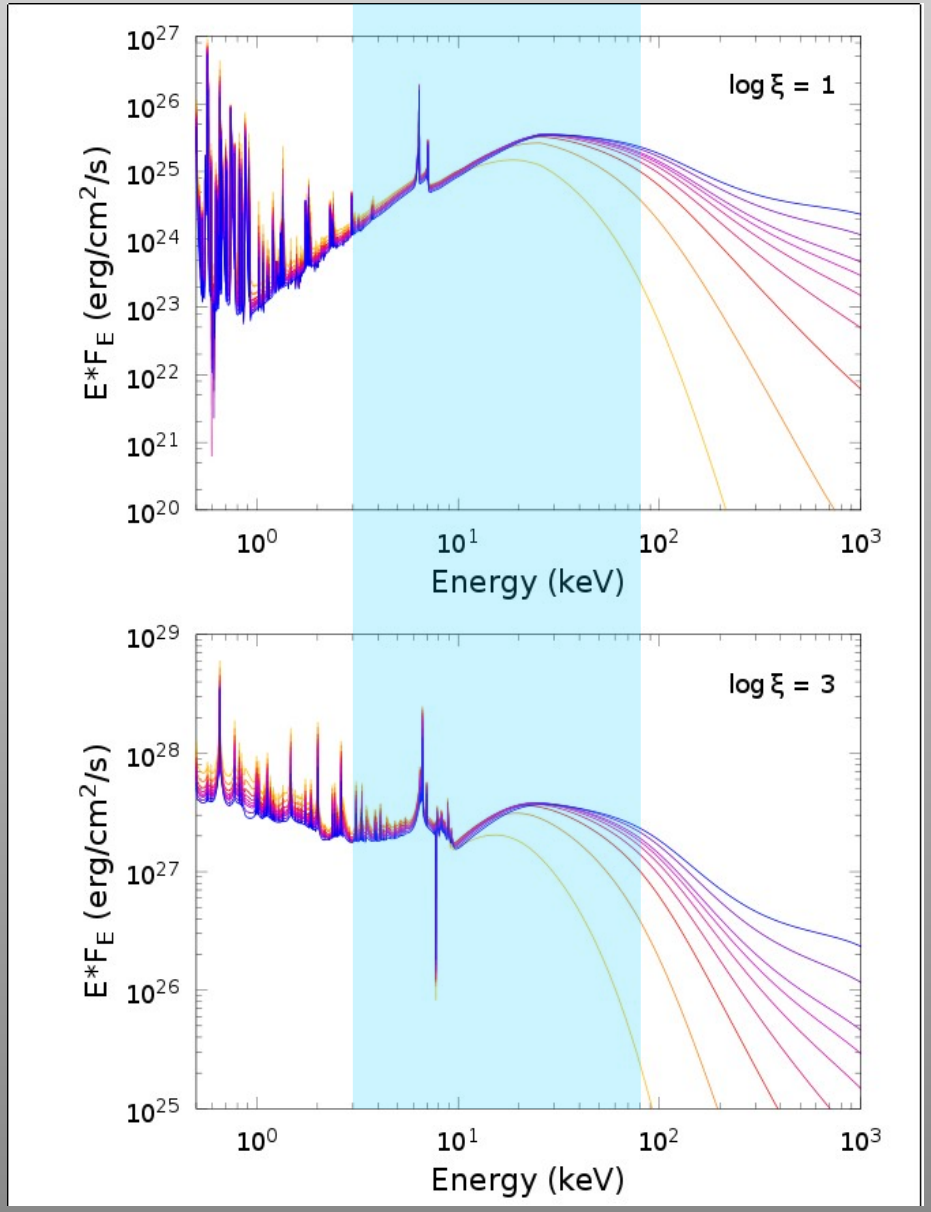

Garcia+15

Introduction

So far, we have only a handful of results based on non focusing, and therefore strongly background-dominated, satellites (BeppoSAX-PDS, Suzaku HXD-PIN, INTEGRAL, Swift-BAT)

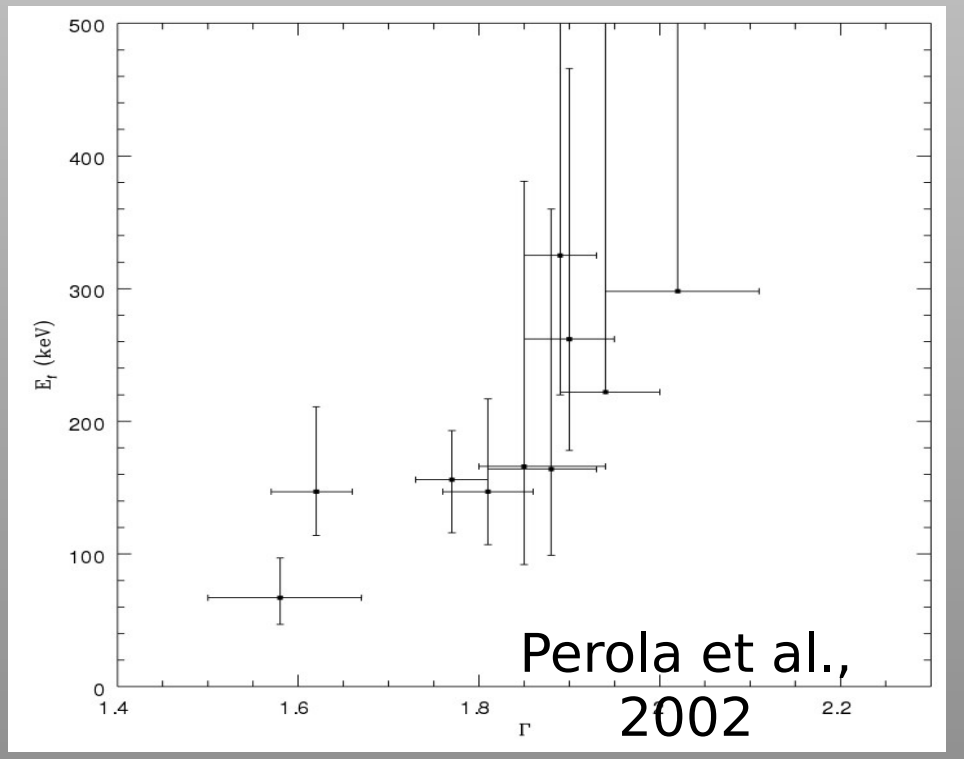

Perola et al., 2002

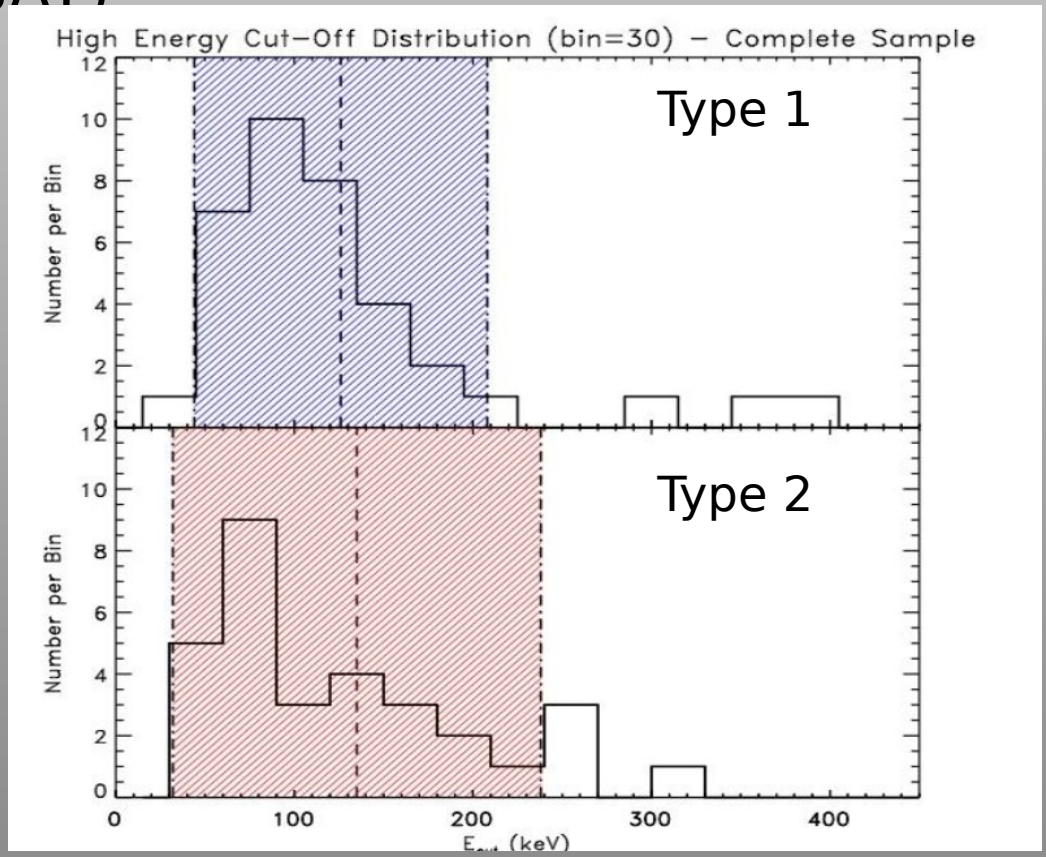

De Rosa et al., 2012; Molina et al., 2013

- Brief introduction on high-energy cutoff measurements
- Nearby AGN seen by NuSTAR
- Results
- Conclusions and future perspectives

Nearby AGN seen by NuSTAR

Source	z	$\log(M)$ $[M_\odot]$	r_{co} $[r_G]$	F_x	E_{cut} [keV]	Γ	Θ	ℓ	Data	References
NGC 5506	0.006	8 ± 1	10	2.9	720^{+130}_{-190}	$1.91^{+0.03}_{-0.03}$	$0.71^{+0.13}_{-0.36}$	4^{+33}_{-3}	SWIFT/NU	1 – 2
NGC7213	0.006	$7.98^{+0.22}_{-0.24}$	10	0.71	> 240	$1.84^{+0.03}_{-0.03}$	> 0.05	$1.0^{+0.7}_{-0.4}$	NU	3 – 4
MCG-6-30-15	0.008	6.7 ± 1	2.9	8.2	> 110	$2.061^{+0.005}_{-0.005}$	> 0.04	258^{+2323}_{-232}	XMM/NU	5 – 6
NGC 2110	0.008	8.3 ± 1	10	8.9	> 210	$1.64^{+0.03}_{-0.03}$	> 0.07	10^{+89}_{-9}	SWIFT/NU	7 – 8
MCG 5-23-16	0.009	7.85 ± 1	10	4.2	116^{+6}_{-5}	$1.85^{+0.01}_{-0.01}$	$0.11^{+0.01}_{-0.04}$	15^{+136}_{-14}	NU	9 – 11
SWIFT J2127.4+5654	0.014	7.18 ± 1	13	1.1	108^{+11}_{-10}	$2.08^{+0.01}_{-0.01}$	$0.11^{+0.01}_{-0.04}$	34^{+308}_{-31}	XMM/NU	12 – 13
IC4329A	0.016	8.1 ± 1	10	4.9	186^{+14}_{-14}	$1.73^{+0.01}_{-0.01}$	$0.18^{+0.01}_{-0.07}$	41^{+365}_{-37}	SU/NU	14 – 15
NGC 5548	0.018	$7.59^{+0.24}_{-0.21}$	4.5	1.3	70^{+40}_{-10}	$1.49^{+0.05}_{-0.05}$	$0.07^{+0.04}_{-0.03}$	88^{+55}_{-37}	XMM/NU	5, 16 – 17
Mrk 335	0.026	$7.42^{+0.12}_{-0.16}$	3	0.10	> 174	$2.14^{+0.02}_{-0.04}$	> 0.06	36^{+16}_{-9}	SWIFT/NU	18 – 19
Ark 120	0.033	$7.66^{+0.05}_{-0.06}$	4.4	0.55	> 68	$1.73^{+0.02}_{-0.02}$	> 0.06	4^{+1}_{-1}	XMM/NU	20 – 21
1H0707-495	0.041	6.31 ± 1	2	0.14	> 63	$3.2^{+0.2}_{-0.2}$	> 0.02	358^{+3219}_{-322}	SWIFT/NU	22 – 23
Fairall 9	0.047	$8.41^{+0.11}_{-0.09}$	21	0.87	> 242	$1.96^{+0.01}_{-0.02}$	> 0.08	12^{+3}_{-3}	XMM/NU	20, 24
3C390.3	0.056	$9.40^{+0.05}_{-0.06}$	10	1.6	116^{+24}_{-8}	$1.70^{+0.01}_{-0.01}$	$0.11^{+0.02}_{-0.04}$	18^{+3}_{-2}	SU/NU	25 – 26
Cyg A	0.056	$9.40^{+0.11}_{-0.14}$	10	1.1	> 110	$1.47^{+0.13}_{-0.06}$	> 0.04	6^{+2}_{-1}	NU	27 – 28
3C382	0.058	9.2 ± 0.5	10	1.4	214^{+147}_{-63}	$1.68^{+0.03}_{-0.02}$	$0.21^{+0.14}_{-0.11}$	12^{+25}_{-8}	SWIFT/NU	29 – 30

F_x is the 0.1-200 keV X-ray flux in 10^{-10} erg cm^{-2} s^{-1}.

References: 1 Guainazzi et al. (2010), 2 Matt et al. (2015), 3 Ursini et al. (2015b), 4 Blank, Harnett & Jones (2005), 5 Emmanoulopoulos et al. (2014), 6 Marinucci et al. (2014c), 7 Moran et al. (2007), 8 Marinucci et al. (2014a), 9 Ponti et al. (2012), 10 Zoghbi et al. (2014), 11 Baloković et al. (2015), 12 Malizia et al. (2008), 13 Marinucci et al. (2014b), 14 Bianchi et al. (2009), 15 Brenneman et al. (2014), 16 Pancoast et al. (2014), 17 Ursini et al. (2015a), 18 Grier et al. (2012), 19 Parker et al. (2014), 20 Peterson et al. (2004), 21 Matt et al. (2014), 22 Bian & Zhao (2003), 23 Kara et al. (2015), 24 Lohfink & Reynolds (2015), 25 Grier et al. (2013), 26 Lohfink & Tombesi (2015), 27 Tadhunter et al. (2003), 28 Reynolds et al. (2015), 29 Winter et al. (2009), 30 Ballantyne et al. (2014)

Fabian+15

- Brief introduction on high-energy cutoff measurements
- Nearby AGN seen by NuSTAR
- Results
- Conclusions and future perspectives

Swift J2127.4+5654

NLS1 with a relativistically broadened Fe Kα emission line (a=0.6±0.2), a steep continuum (Γ=2-2.4), E_c=30-90 keV, L_{bol}/L_{Edd}~0.18 (Miniutti+09, Malizia+08, Panessa+11, Sanfrutos+13)

It was observed simultaneously with XMM-Newton for ~300 ks and both a strong Compton Hump and a broad Fe Kα line are present

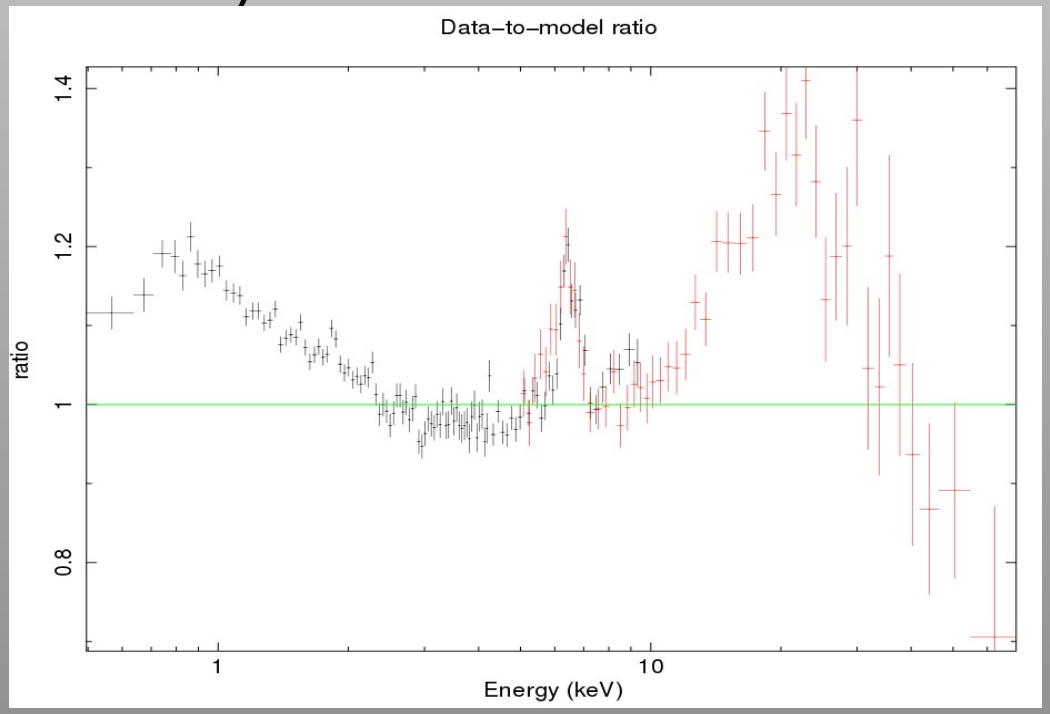

Swift J2127.4+5654

When a model composed of a primary continuum, relativistic and distant reflection components is applied to the data the only residuals are above ~25 keV

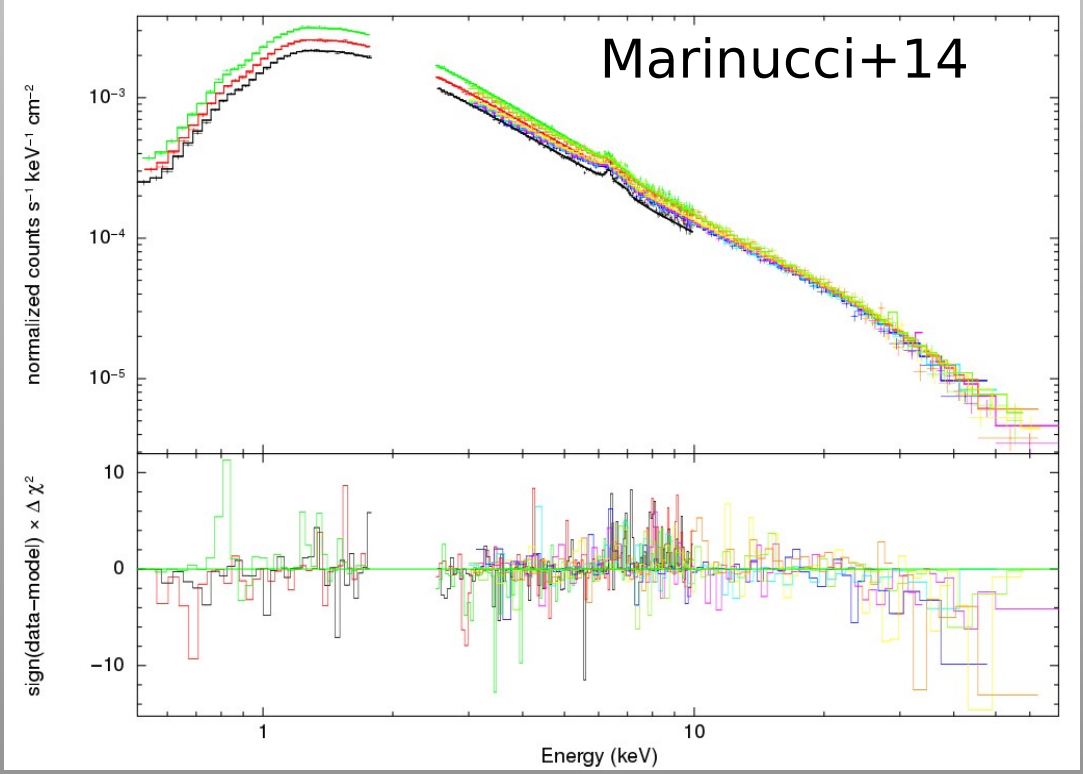

Swift J2127.4+5654

When a model composed of a primary continuum, relativistic and distant reflection components is applied to the data the only residuals are above ~25 keV

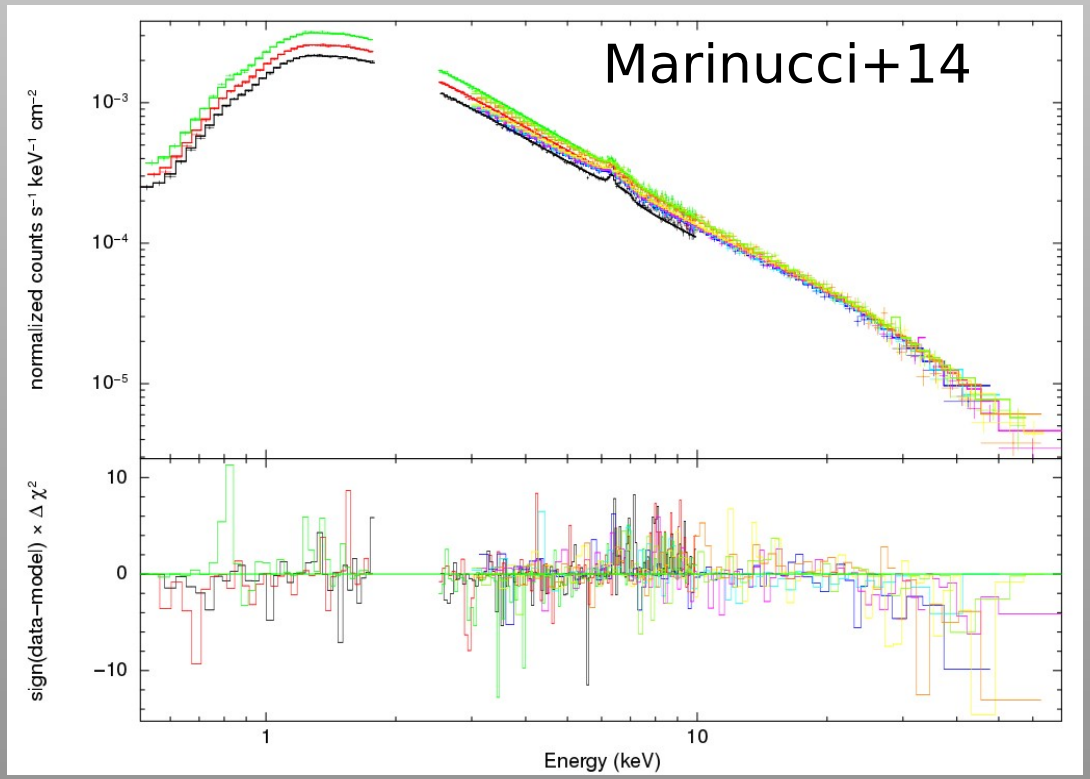

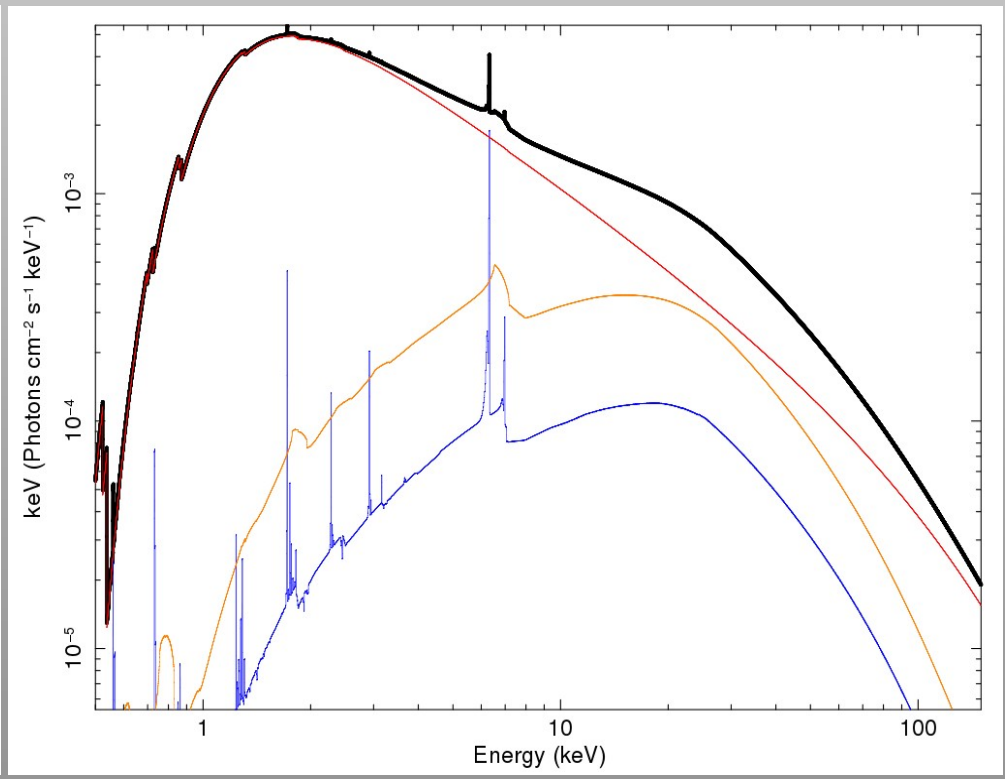

The inclusion of relxill model (Garcia & Dauser +14) allows us to measure a cutoff energy E_c=108±10 keV and to infer the contribution of the disk to the Compton hump.

Swift J2127.4+5654

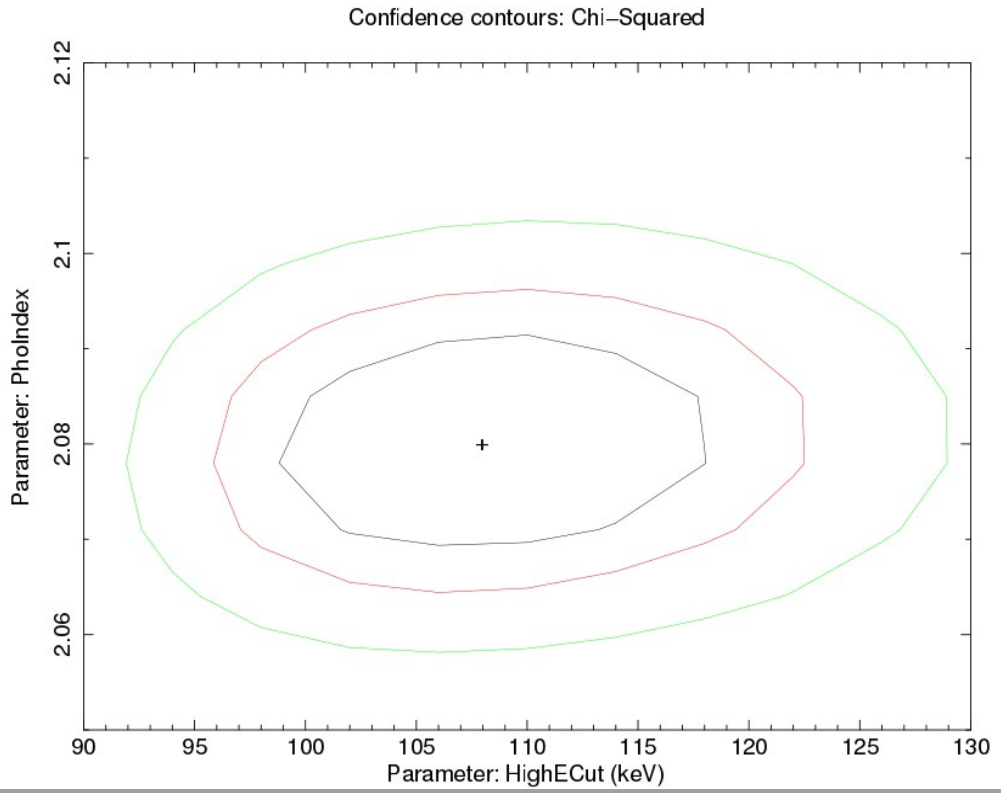

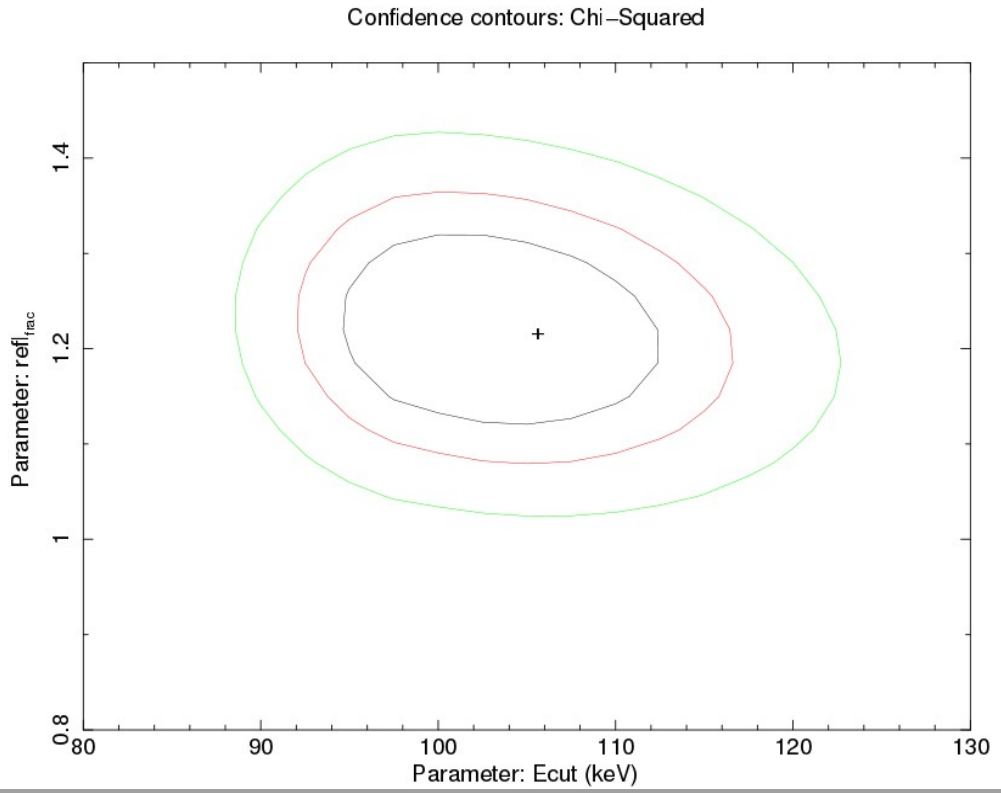

Using compTT (Titarchuk+94) with two different geometries we get:

SLAB

$kT_e = 68^{+37}_{-32}$ keV

$\tau = 0.35^{+0.35}_{-0.19}$

SPHERE

$kT_e = 53^{+28}_{-26}$ keV

$\tau = 1.35^{+1.03}_{-0.67}$

MCG-05-23-16

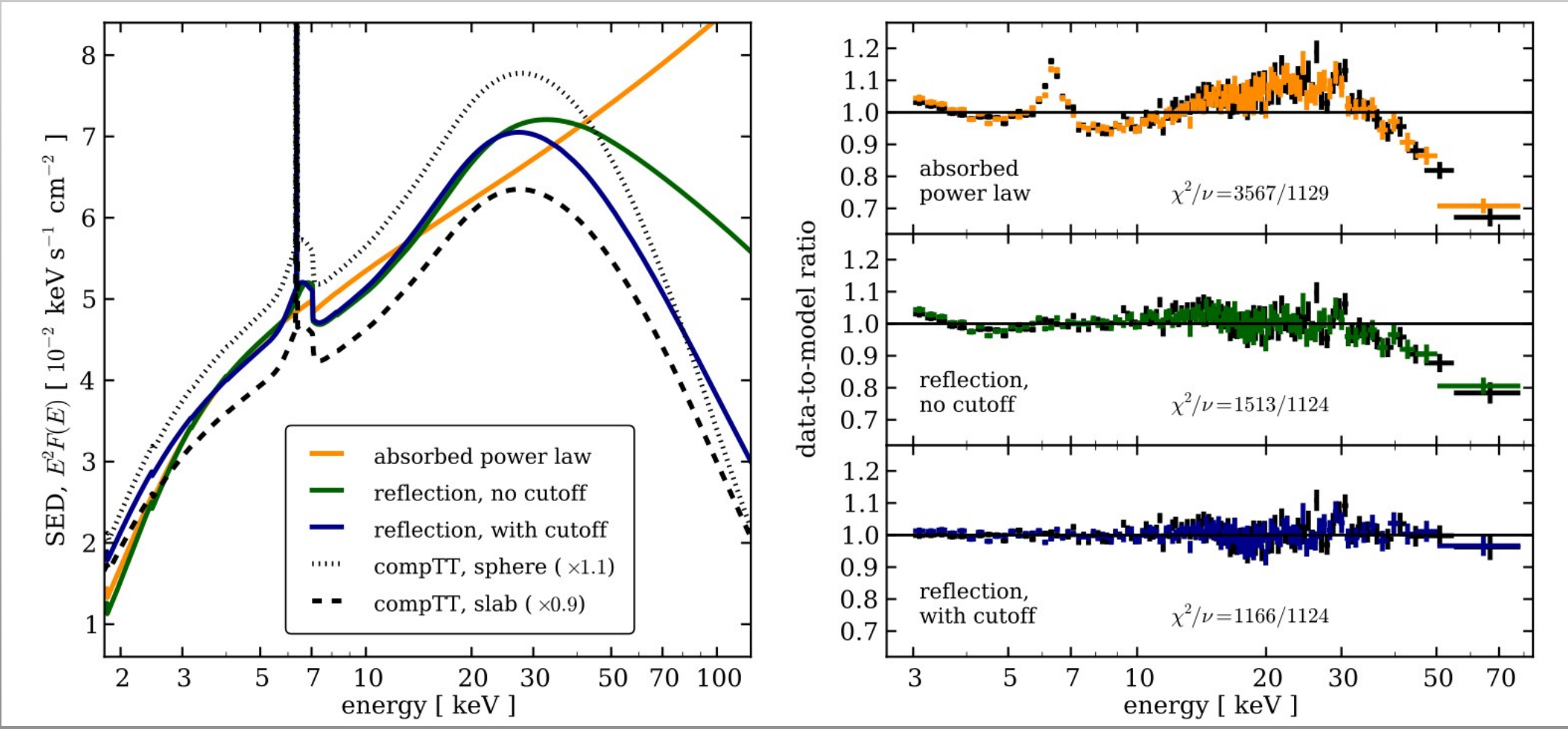

Balokovic+15

MCG-05-23-16

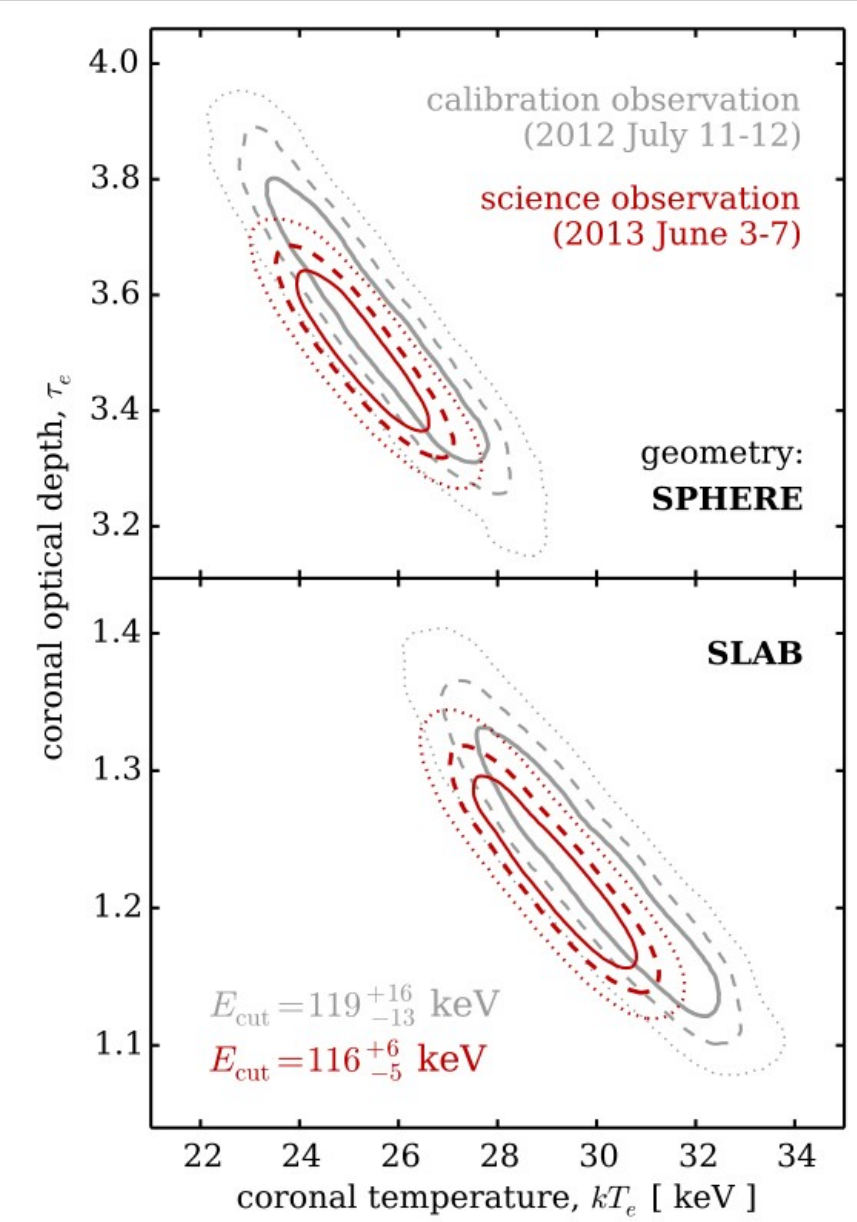

Balokovic et al. 2015

independent of the continuum model			
$C_{\rm FPMB}$ [c]		1.032 ± 0.002	1.045 ± 0.005
$E_{\rm line\,1}$	[keV]	6.43 ± 0.05	$6.5^{+0.2}_{-0.1}$
$\sigma_{\rm line\,1}$	[keV]	0.46 ± 0.06	0.5 ± 0.2
$\rm EW_{line\,1}$	[eV]	80 ± 10	80 ± 20
$\rm EW_{line\,2}$	[eV]	40 ± 10	50 ± 20
phenomenological continuum model: `pexrav`			
χ^2		1163	687
Γ		1.85 ± 0.01	1.83 ± 0.02
R		0.87 ± 0.04	1.1 ± 0.1
$E_{\rm cut}$	[keV]	116^{+6}_{-5}	119^{+16}_{-13}
Comptonized continuum model: `refl(compTT)`			
assumed corona geometry: slab			
χ^2		1163	688
R		0.84 ± 0.04	1.1 ± 0.1
kT_e	[keV]	29 ± 2	30 ± 3
τ_e		1.23 ± 0.08	1.2 ± 0.1
assumed corona geometry: sphere			
χ^2		1161	688
R		0.82 ± 0.04	1.0 ± 0.1
kT_e	[keV]	25 ± 2	26 ± 3
τ_e		3.5 ± 0.2	3.5 ± 0.3

High values/lower limits

In other bright sources, high values or lower limits to the cutoff energy have been found, suggesting the presence of a very hot corona surrounding the accretion disc.

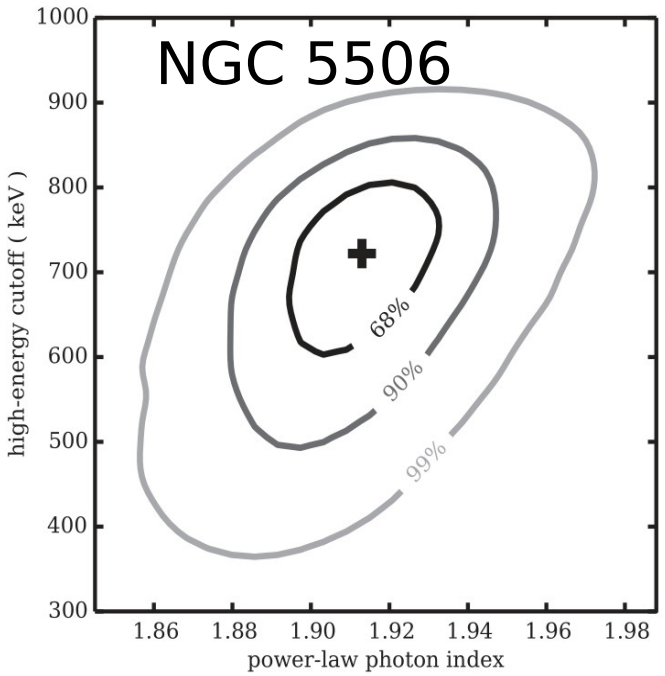

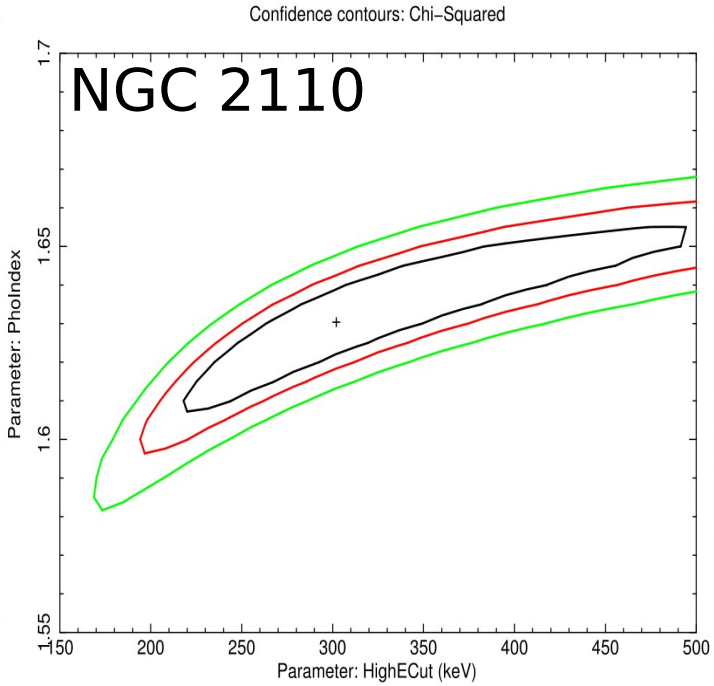

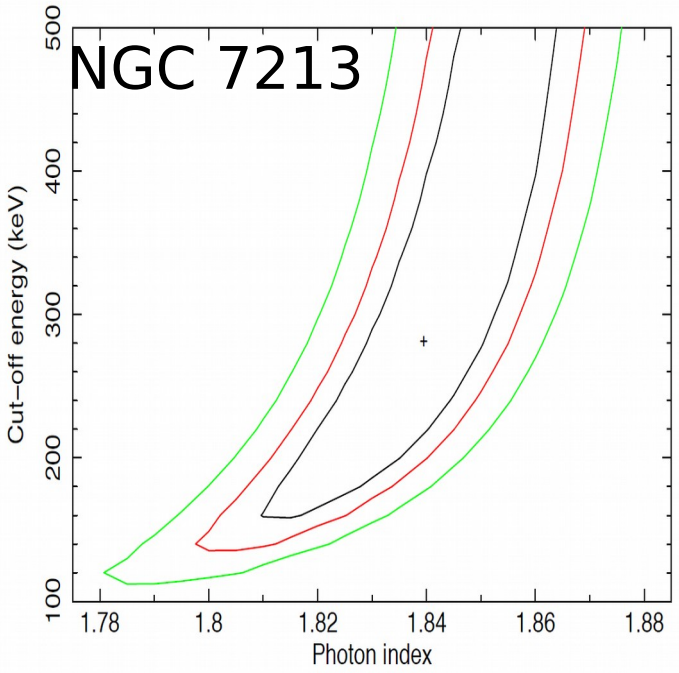

Matt+2015

Marinucci+2015

Ursini+subm.,
see Tortosa's poster

The next step is to build a small catalog and to start looking for correlations between the coronal temperature and other physical properties (e.g. black hole mass, accretion rate).

A larger view

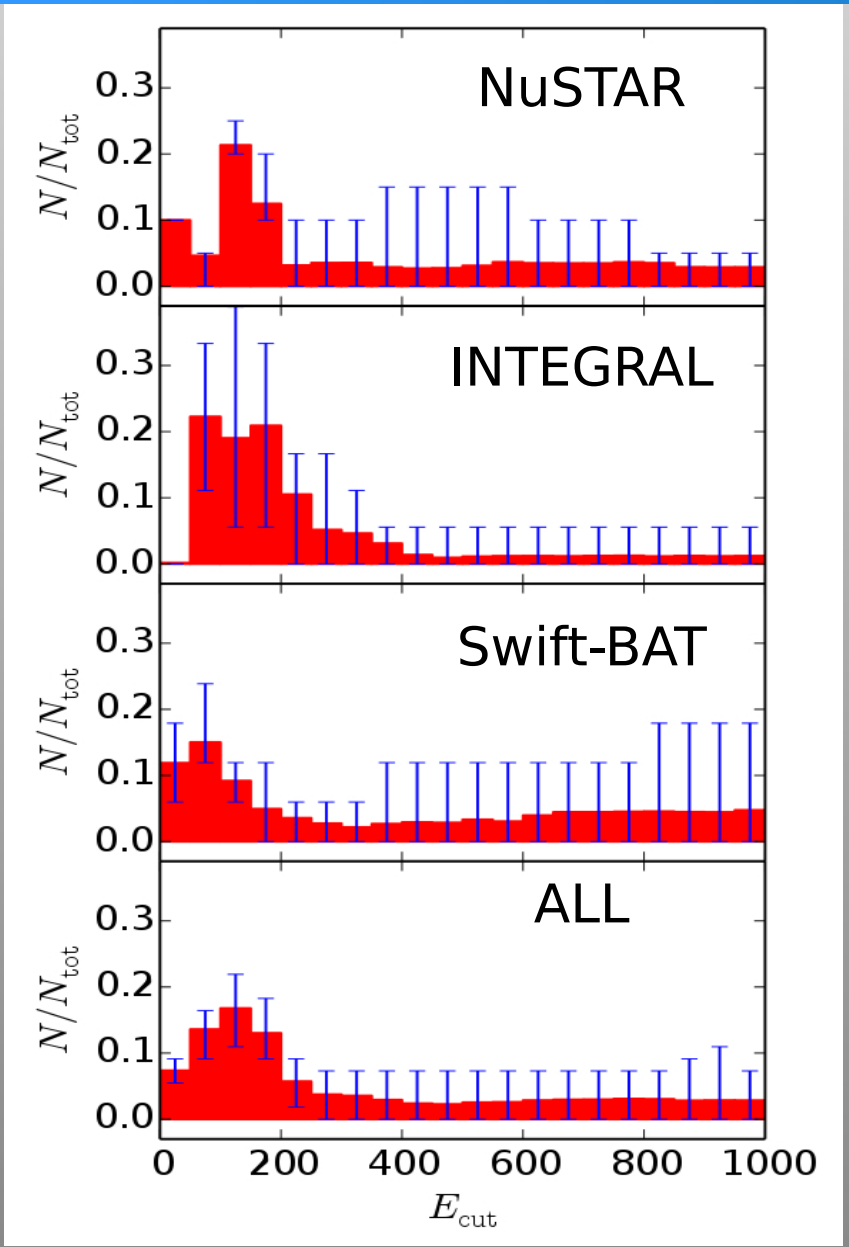

Fabian+1

A larger view

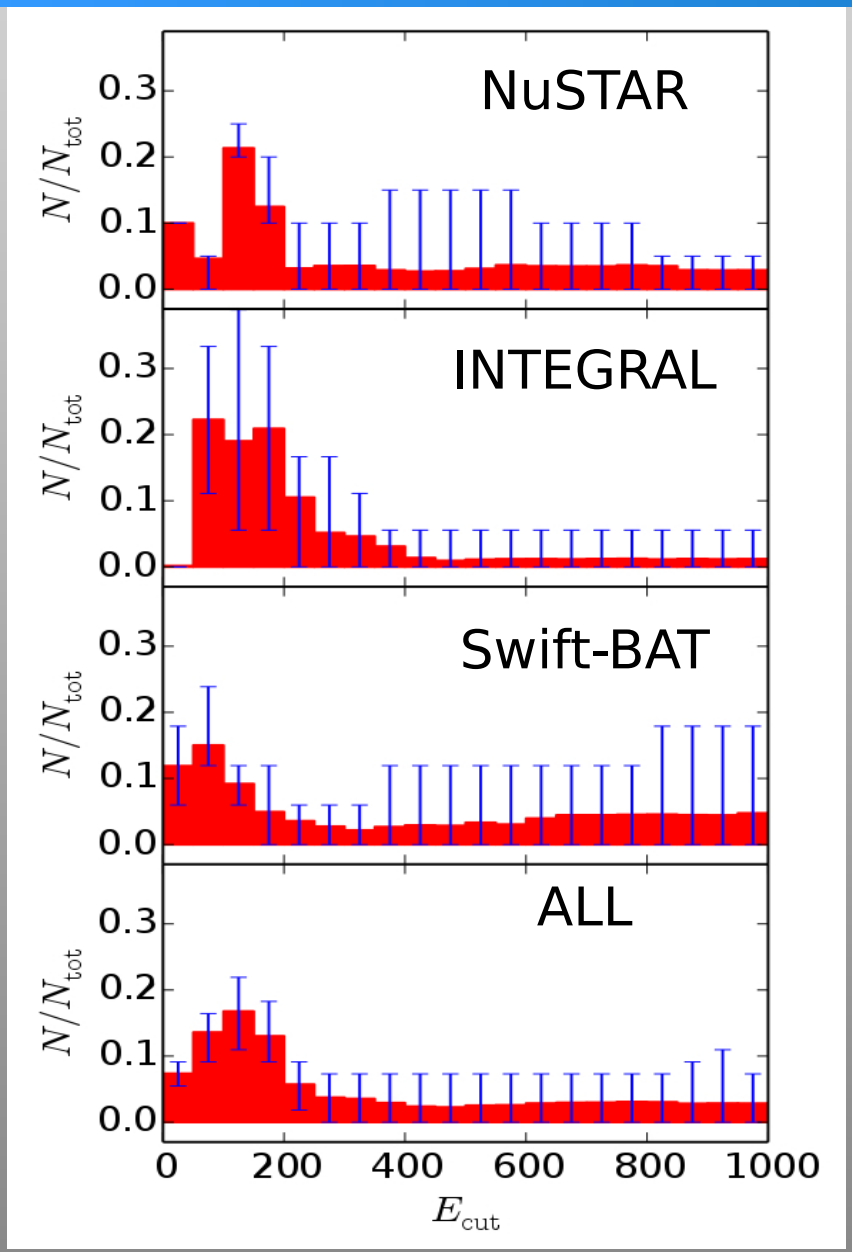

Fabian+1

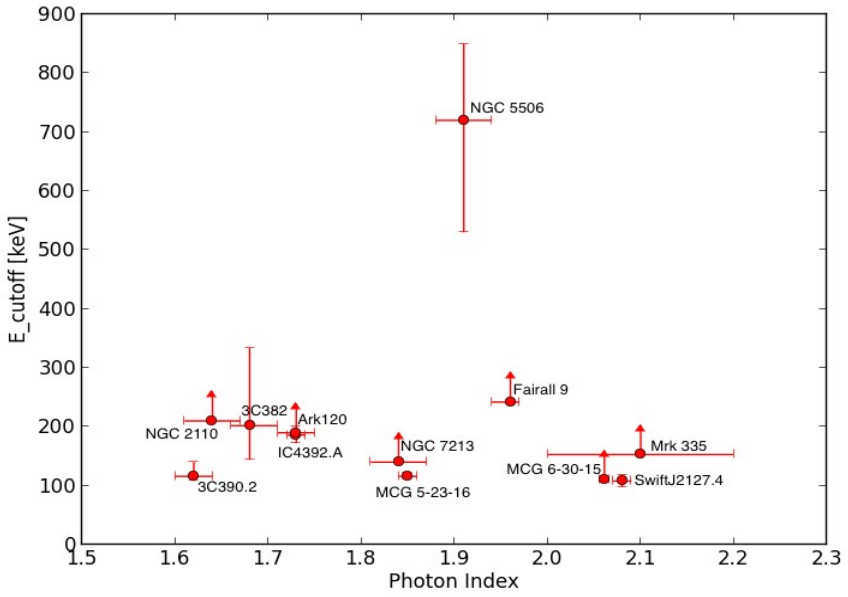

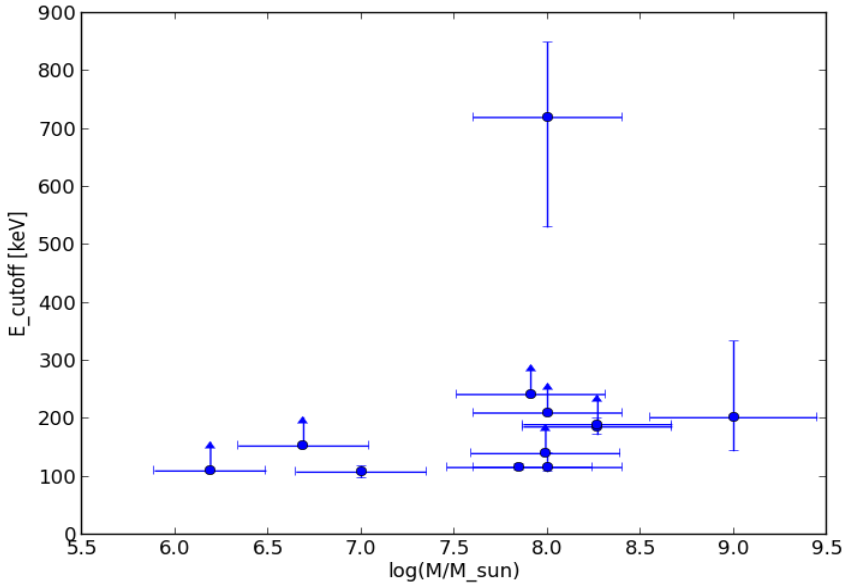

Tortosa et al., in prep.

- Brief introduction on high-energy cutoff measurements
- Nearby AGN seen by NuSTAR
- Results
- Conclusions and future perspectives

Conclusions

- High energy cut-off have been measured in a number of AGN with NuSTAR (more are yet to come!)

- They are not ubiquitous

- The hard X-ray band (3-80 keV) is fundamental for testing and discriminating between different Comptonization models

- Further observations will help us in understanding the nature of the primary continuum, such as the relation between the accretion rate and the cutoff energy and the link between the disc reflection and the extension of the hot corona.